

UCLA

UCLA Previously Published Works

Title

Effects of cranial electrotherapy stimulation on resting state brain activity.

Permalink

<https://escholarship.org/uc/item/6gs5p1pb>

Journal

Brain and behavior, 2(3)

ISSN

2162-3279

Authors

Feusner, Jamie D
Madsen, Sarah
Moody, Teena D
et al.

Publication Date

2012-05-01

DOI

10.1002/brb3.45

Peer reviewed

Effects of cranial electrotherapy stimulation on resting state brain activity

Jamie D. Feusner¹, Sarah Madsen¹, Teena D. Moody¹, Cara Bohon¹, Emily Hembacher², Susan Y. Bookheimer³ & Alexander Bystritsky¹

¹Department of Psychiatry and Biobehavioral Sciences, David Geffen School of Medicine, University of California, Los Angeles, California

²Department of Psychology, University of California, Davis, California

³Center for Cognitive Neuroscience, Semel Institute for Neuroscience and Human Behavior, University of California, Los Angeles, California

Keywords

CES, default mode network, fMRI, fronto-parietal network, intrinsic connectivity networks, sensorimotor network.

Correspondence

Jamie D. Feusner, Department of Psychiatry and Biobehavioral Sciences, David Geffen School of Medicine, 300 UCLA Medical Plaza, Suite 2200, Los Angeles, CA 90095.
Tel: +1 310 206 4951; Fax: +1 323 443 3593;
E-mail: jfeusner@mednet.ucla.edu

Funded by a grant from the Saban Family Foundation (Dr. Bystritsky). Also supported by a grant from the National Institute of Mental Health (5K23 MH079212 – Dr. Feusner).

Received: 27 January 2012;

Accepted: 10 February 2012

Brain and Behavior 2012; 2(3): 211–220

doi: 10.1002/brb3.45

Abstract

Cranial electrotherapy stimulation (CES) is a U.S. Food and Drug Administration (FDA)-approved treatment for insomnia, depression, and anxiety consisting of pulsed, low-intensity current applied to the earlobes or scalp. Despite empirical evidence of clinical efficacy, its mechanism of action is largely unknown. The goal was to characterize the acute effects of CES on resting state brain activity. Our primary hypothesis was that CES would result in deactivation in cortical and subcortical regions. Eleven healthy controls were administered CES applied to the earlobes at subsensory thresholds while being scanned with functional magnetic resonance imaging in the resting state. We tested 0.5- and 100-Hz stimulation, using blocks of 22 sec “on” alternating with 22 sec of baseline (device was “off”). The primary outcome measure was differences in blood oxygen level dependent data associated with the device being on versus baseline. The secondary outcome measures were the effects of stimulation on connectivity within the default mode, sensorimotor, and fronto-parietal networks. Both 0.5- and 100-Hz stimulation resulted in significant deactivation in midline frontal and parietal regions. 100-Hz stimulation was associated with both increases and decreases in connectivity within the default mode network (DMN). Results suggest that CES causes cortical brain deactivation, with a similar pattern for high- and low-frequency stimulation, and alters connectivity in the DMN. These effects may result from interference from high- or low-frequency noise. Small perturbations of brain oscillations may therefore have significant effects on normal resting state brain activity. These results provide insight into the mechanism of action of CES, and may assist in the future development of optimal parameters for effective treatment.

Introduction

Cranial electrotherapy stimulation (CES) is a noninvasive therapeutic device that applies pulsed, alternating microcurrent ($<1000 \mu\text{A}$) transcutaneously to the head via electrodes placed on the earlobes, mastoid processes, zygomatic arches, or the maxillo-occipital junction. The U.S. Food and Drug Administration (FDA) granted approval in 1979 for CES for the treatment of insomnia, depression, and anxiety, and it is commercially available for personal use. Controlled studies provide evidence that CES is effective for anxiety, headaches, fibromyalgia, smoking cessation, drug withdrawal symp-

toms, and (in some but not all studies) pain (see Bianco 1994; Klawansky et al. 1995; Kirsch 1996; DeFelice 1997; Gilula 2007; O'Connell et al. 2010 for review and meta-analyses). The majority of controlled studies have evaluated the efficacy of CES for treatment of anxiety, although most were performed in nonclinical samples (Klawansky et al. 1995; DeFelice 1997). However, in a six-week open-label pilot study of treatment of individuals with generalized anxiety disorder (GAD), CES applied to the earlobes was found to reduce symptoms of GAD, as demonstrated by a significant mean 40.4% decrease in Hamilton Anxiety Rating Scale scores at endpoint compared to baseline (Bystritsky et al. 2008).

Despite empirical evidence for treatment efficacy for these syndromes, skepticism remains as to how application of microcurrent to the earlobes or scalp could effect these clinical changes, likely because of the dearth of studies of its mechanism. As brain stimulation techniques increasingly hold promise for treatment of neurological and psychiatric disorders (George et al. 2007), better understanding of their mechanisms of action is crucial to further improve their efficacy, develop new technologies, and evaluate their safety.

It remains unclear how the electrical current from CES may alter brain activity. Forty-two to 46% of the applied CES current enters the brain, with the highest levels of current recorded in the thalamus (Rush and Driscoll 1968; Jarzembowski and Sances 1970). One theory suggests that the cranial alternating current (AC) stimulation interferes with ongoing brain wave oscillations by introducing cortical noise (Zaghi et al. 2009). In vitro studies of rat brain slices show that high-frequency (50–200 Hz) sinusoidal AC stimulation suppresses activity in cell bodies and axons (Jensen and Durand 2007). Perhaps the most investigated effects to date of CES have come from electroencephalographic (EEG) studies, which have found recordings to be altered during and after treatment with CES. Alpha EEG waves were slowed following CES in monkeys, and this change was associated with a reduction in adverse reactions to stressful stimuli (Jarzembowski 1985). Applying CES at 0.5- and 100-Hz with simultaneous EEG resulted in a downward shift in mean alpha frequency, with greater effect for 100-Hz stimulation (Schroeder and Barr 2001). CES also results in a decrease in alpha band median frequency and beta band power fraction (Itil et al. 1972). These changes are similar to EEG changes in trained meditators, and may be associated with a relaxed state (Banquet 1973). Although it remains unclear if these alterations in brain wave oscillation patterns are a cause or effect of improved clinical states, pulsed current may interrupt nervous system function.

The goal of this study was to determine the immediate effects of CES stimulation on patterns of brain activity in the resting state, and on functional connectivity within intrinsic connectivity networks. This represents the first investigation of the direct effects of CES on brain activity using functional neuroimaging simultaneously with cranial stimulation. We hypothesized that CES would result in deactivation in cortical and subcortical (thalamic) regions, in line with evidence that stimulation interferes with oscillatory brain activity and is associated with reduction of brain wave frequencies (mean alpha power). We also predicted that 0.5- versus 100-Hz stimulation would result in different patterns. In addition, we hypothesized that stimulation would alter intrinsic connectivity networks such as the dorsal fronto-parietal network (FPN) (Corbetta and Shulman 2002) (due to evidence of improvements in attention with CES [Southworth 1999]), and the sensorimotor network (SMN) (Mantini et al. 2007; Schopf

et al. 2010) (due to evidence of clinical efficacy for pain [Tan et al. 2011]). We also predicted it would alter connectivity within the default mode network (DMN), as the EEG beta band (which CES 100 Hz may affect [Schroeder and Barr 2001]) has been found to correlate with this network (Mantini et al. 2007; Laufs 2008).

Material and Methods

Participants

The UCLA Institutional Review Board approved the study protocol. Informed consent was obtained after the nature and possible consequences of the studies were explained.

Eleven healthy right-handed male and female participants aged 18–65 were recruited from the community. We administered the Mini International Neuropsychiatric Interview (MINI) (Sheehan et al. 1998) and excluded participants if they met Diagnostic and Statistical Manual of Mental Disorders (DSM-IV) criteria for any Axis I psychiatric disorder including active substance abuse, and any participants whom the investigator judged were suicidal. Other exclusion criteria included any neurological disorders or any medical disorders that could affect cerebral metabolism. Participants were excluded if they were taking any psychotropic medications or any other medications with psychoactive properties. Pregnant or breastfeeding women and those of childbearing potential who were not practicing a reliable form of contraception were also excluded from the study. Due to constraints of magnetic resonance imaging (MRI) scanning, we excluded individuals who weighed greater than 280 lbs and those with implanted electronic devices or ferromagnetic materials.

CES device

We used the Alpha-Stim[®] 100 microcurrent and cranial electrotherapy stimulator for the experiment, provided by the manufacturer Electromedical Products, International (Mineral Wells, TX). The AlphaStim[®] 100 provides cranial electrical stimulation by generating bipolar asymmetric rectangular waves with a frequency of 0.5, 1.5, or 100 Hz, and a current intensity that can be adjusted continuously to provide between 10 and 600 μ A (<http://www.alpha-stim.com>). We tested 0.5- and 100-Hz pulse frequencies, as these are most commonly used in clinical treatment. For the purpose of the experiment, the manufacturer modified the device to automatically cycle between “on” blocks of 22 sec (specifically 10 sec on, then 2 sec off, then 10 sec on, due to constraints of the device) and “off” blocks of 22 sec. The device was connected via copper wires to adhesive nonferromagnetic electrodes (1.5-cm diameter contact area) that were placed on the participants’ right and left earlobes.

Pre-MRI sensory threshold CES testing

Participants received individualized subsensory current intensities to minimize the possibility that the current could be felt consciously in the scanner. This was done in order to avoid activation patterns associated with perception of stimulation, and also conforms to the way the device is used clinically. Testing was done using a forced-choice test outside of the scanner, to ensure that the participants could not guess if the device was on or off, at greater than chance level (see Supporting Information for details).

CES safety testing in the MR environment

Prior to the experiment, we tested the use of CES in the MRI scanner to ensure safety in terms of current, voltage, and temperature, and to verify that it did not produce any artifacts or field inhomogeneities in the MR image (see Supporting Information for details).

Behavioral measurements

To assess for any changes in anxiety related to CES stimulation, participants completed the state portion of the State-Trait Anxiety Inventory (STAI) (Spielberger et al. 1983) before and after the fMRI scan.

fMRI

Participants were positioned in the scanner and the electrodes were applied to their earlobes. These were connected via long copper wires to the CES device, which the investigator operated in the scanner control room. Participants were instructed to: “keep your eyes closed for the duration of the scan but try not to fall asleep. You do not have to think about anything in particular.” After the scan, they were informally questioned about whether they could feel the stimulation during the scan.

The experiment consisted of a blocked design in which six “on” blocks of 22 sec alternated with six “off” blocks of 22 sec. There was 37.5 sec of baseline prior to the “on” and “off” cycles, and 33.5 sec of baseline following it. The total duration of each experimental run was 5 min and 35 sec. Participants completed one run each of the 0.5- and 100-Hz pulse frequencies, the order of which was counterbalanced between participants. Although the investigator in the control room knew when the CES was cycling between “on” and “off” during the scan, the participants did not have any contact with him during each experimental run, and therefore could not be influenced implicitly or explicitly by the investigator’s knowledge. In this way, a control condition was built into the experiment in which there were blocks when the CES was off, but the participants did not know when this was occurring.

We used a 3-Tesla Trio (Siemens) MRI scanner to evaluate BOLD contrast, using T2*-weighted echo planar imaging

(EPI) gradient-echo pulse sequence (repetition time (TR) = 2.5 sec, echo time (TE) = 21 msec, flip angle = 75°, matrix = 64 × 64, field-of-view = 24 × 24 cm, in-plane voxel size 3.1 × 3.1 mm, slice thickness 3 mm, 1-mm intervening spaces, and 34 total slices). We obtained matched-bandwidth T2-weighted images for functional image registration. We also obtained higher resolution T1-weighted three-dimensional magnetic resonance images with 1-mm³ voxel size for each participant to provide detailed brain anatomy. For these, magnetization-prepared rapid gradient echo (MP-RAGE) sequences were used, with the parameters: TE = 2.26 msec, TR = 1900 msec, TI = 900 msec, flip angle = 9.00°, field-of-view = 240 × 256, matrix = 240 × 256, slice thickness = 1 mm, 176 slices.

Image processing included motion correction, skull stripping, spatial smoothing of 5-mm full-width/half-maximum Gaussian kernel, mean-based intensity normalization of all volumes by the same factor, and high-pass temporal filtering. We coregistered functional images of each participant to corresponding matched-bandwidth structural images in native space, then performed a second-stage registration to their MP-RAGE scans, and finally registered these to structural standard images, defined by the Montreal Neurological Institute averaged 152 standard brain. Registration to high-resolution and standard images was carried out using FLIRT (Jenkinson and Smith 2001; Jenkinson et al. 2002).

Statistical analysis

Voxel-wise analysis

For image analysis, we used FEAT software (FMRI Expert Analysis Tool) Version 5.98, part of the Oxford Centre for Functional Magnetic Resonance Imaging of the Brain Software Library (FSL), www.fmrib.ox.ac.uk/fsl. FMRIB’s Improved Linear Model (FILM) was used for time-series statistical analysis, using local autocorrelation correction (Woolrich et al. 2001). We thresholded Z-statistic images using clusters determined by $Z > 2.3$ and a (corrected) cluster significance threshold of $P = 0.05$ (Worsley 2001).

For the first-level (individual subject) analysis, we modeled the hemodynamic response function using a convolution of the experimental paradigms of each “on” period versus baseline with the canonical hemodynamic response function and its temporal derivative (Aguirre et al. 1998). We analyzed the normalized data using regressors to model hemodynamic changes associated with the contrasts of “on” versus baseline for both the 0.5- and 100-Hz frequencies. For the “on” 22-sec blocks, we modeled only the two 10-sec periods that the device was actually on, and not the 2 sec intervening off period. The baseline consisted of the six “off” blocks plus the 33.5 sec of baseline at the end of the run. We tested both relative activation (modeled as “1”) and deactivation (modeled as “−1”). For the second-level (group) analysis, we combined

data across participants using FLAME 1 + 2 (FMRIB's Local Analysis of Mixed Effects) (Beckmann et al. 2003), with participant as the random factor. We additionally performed a contrast to compare activation associated with the 0.5- versus 100-Hz frequencies.

Region-of-interest (ROI) analysis

To test our hypothesis about the effect of CES on thalamic activity, we used an anatomical mask for the thalamus from the Harvard-Oxford subcortical probabilistic structural atlas supplied with FSL (50% probability mask). We calculated mean percent signal change in each region and compared "on" versus baseline using paired *t*-tests.

Exploratory analysis with current intensity

To investigate the relationship between stimulation current intensity and brain activation patterns, we used participants' individualized current intensities (Table S1) as a regressor in the general linear model.

"On" versus baseline block-by-block analysis

To understand the reliability of the effects on brain activity of the device being "on" versus baseline, we analyzed the percentage BOLD signal change for each "on" block individually, averaged across the regions found to be significantly deactivated from the voxel-wise analysis. To reduce bias for this secondary analysis due to nonindependence, and as an internal cross-validation, we used a leave-one-subject-out (LOSO) method (Esterman et al. 2010) (Fig. S1, and see Supporting Information for methods).

Psychophysiological interaction (PPI) analysis

We investigated functional connectivity in three well-characterized resting state networks: the DMN (Shulman et al. 1997; Buckner et al. 2008), the SMN (Mantini et al. 2007), and the FPN (Sridharan et al. 2008; Spreng et al. 2010). To test how CES affects these networks, we used a psychophysiological interaction (PPI) analysis (Friston et al. 1997). A PPI analysis is a linear regression method that utilizes one regressor to represent the BOLD time course across the brain associated with activation of a seed region (the "physiological" regressor), one regressor that represents the brain activation associated with the device being "on" versus baseline (the "psychological" regressor), and one regressor that is the interaction of the previous two regressors. This third interaction regressor conceptually represents the regions of the brain for which there is increased functional connectivity with the seed region, specifically associated with CES being "on."

We used a 4-mm sphere seed region in bilateral posterior cingulate gyrus (centered at Montreal Neurological Institute (MNI) coordinates $-14, -56, 12$ and $6, -56, 16$ —consistent

with previous studies that identified DMN [De Luca et al. 2006; Uddin et al. 2009]). We used a seed region in bilateral postcentral gyrus (centered at MNI coordinates $-29, -32, 57$ and $33, -29, 56$ —consistent with a previous study that identified SMN [Mantini et al. 2007]). We used a seed region in the inferior parietal lobule (IPL) (centered at MNI coordinates $50, -45, 51$ and $-41, -57, 51$ —consistent with a previous study that identified FPN [Mantini et al. 2007]). To constrain our investigation to other nodes within each network, we used masks created from the Harvard-Oxford Cortical probabilistic atlas supplied with FSL. The DMN mask consisted of the medial prefrontal cortex, the hippocampus, and the IPL (specifically, the angular gyrus and supramarginal gyrus). The SMN mask consisted of the precentral and postcentral gyri, the supplementary motor area (SMA), and the paracalculare cortex. The FPN mask consisted of the precentral gyrus and middle frontal gyrus.

fMRI data processing was carried out using FEAT Version 5.98. Higher level analysis was carried out using OLS (ordinary least squares) simple mixed effects. We thresholded *Z*-statistic images using clusters determined by $Z > 2.0$ and a (corrected) cluster significance threshold of $P = 0.05$ (Worsley 2001). We used a lower statistical threshold ($Z > 2.0$) for the PPI analysis because of the low power inherent to this type of analysis due to possible multicollinearity between the physiological and/or psychological regressors and the interaction term.

Results

Participant demographics (Table S1)

Thirteen participants were initially enrolled. One participant was disqualified because he could feel the stimulation at the lowest possible current of $10 \mu\text{A}$. Another potential participant was unable to perform the fMRI experiment due to claustrophobia. Data were therefore collected and analyzed for eleven participants.

Behavioral data (Table S1)

Mean ratings on the STAI did not differ significantly before and after the experiment (before: 21.9 ± 3.9 ; after: 22.6 ± 3.1 ; $t_{18} = .428$ $P = .674$). Only one participant reported awareness of any sensation during the scan; she felt a constant "sensation" on her left earlobe during the entire duration of the scan, at the location where the headphones pressed on her earlobe (but not at the electrode site).

"On" versus baseline voxel-wise analysis (Figs. 1, 2 and Table 1)

At both frequencies, participants exhibited deactivation in frontal, parietal, and posterior midline regions. A total of 0.5-Hz stimulation was associated with decreased activation

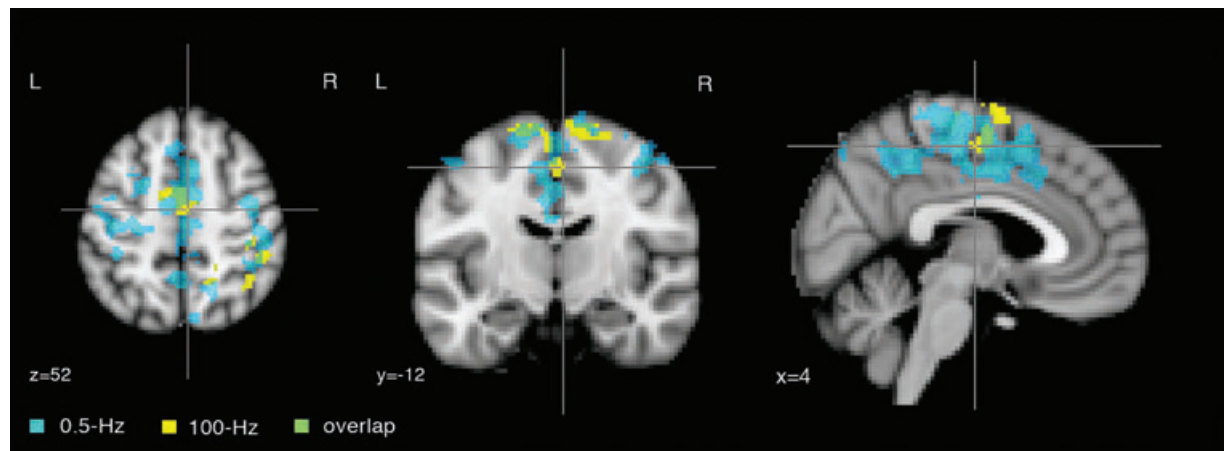


Figure 1. Regions of decreased brain activity as a result of cranial electrotherapy stimulation (CES) for 0.5-Hz stimulation (blue), 100-Hz stimulation (yellow), and regions of overlap between the two frequencies (green).

in regions including the left SMA, bilateral precentral and postcentral gyri, right posterior cingulate cortex, right lateral occipital cortex, and bilateral precuneus. A total of 100-Hz stimulation was associated with decreased activation in

regions including the right/left SMA, right supramarginal gyrus, right superior parietal lobule, and left superior frontal gyrus. There were no regions of increased activation for either frequency. A direct comparison of 0.5- and 100-Hz

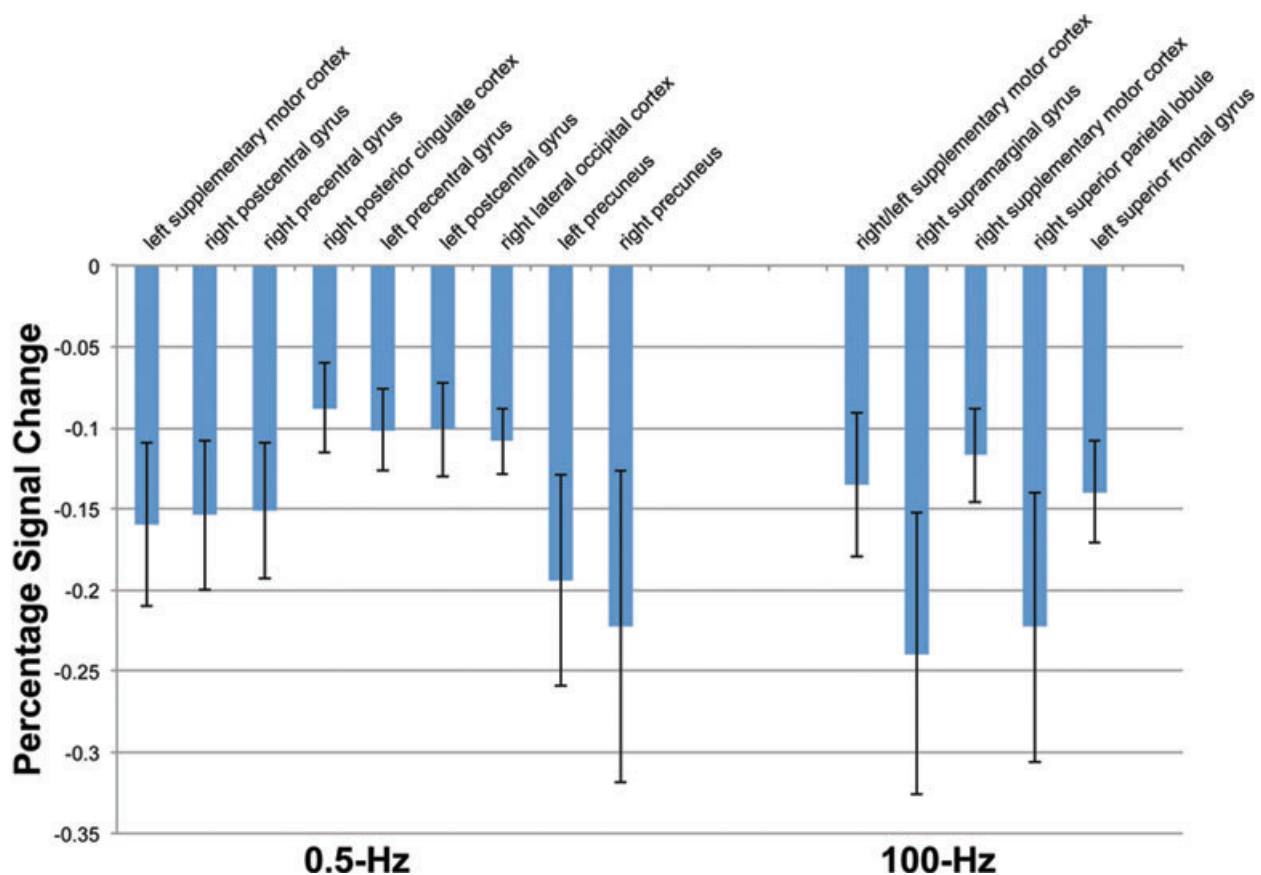


Figure 2. Regional brain deactivation (BOLD percentage signal change \pm SEM) associated with 0.5- and 100-Hz "on" CES stimulation versus baseline, based on local maxima from the voxel-wise analysis.

Table 1. Local maxima for regional deactivation from cranial electrotherapy stimulation (CES).

		MNI coordinates		
	Z score	x	y	z
0.5 Hz				
Left supplementary motor cortex	3.73	−2	−4	56
Right postcentral gyrus	3.66	44	−30	48
Right precentral gyrus	3.57	42	−10	56
Right posterior cingulate cortex	3.47	16	−40	38
Left precentral gyrus	3.37	−24	−24	54
Left postcentral gyrus	3.36	−40	−24	46
Right lateral occipital cortex	3.35	18	−70	46
Left precuneus	3.33	−2	−74	44
Right precuneus	2.75	6	−76	50
100 Hz				
Right/left supplementary motor cortex	3.61	0	−6	58
Right supramarginal gyrus	3.45	46	−38	56
Right supplementary motor cortex	3.34	8	2	64
Right superior parietal lobule	3.32	24	−52	70
Left superior frontal gyrus	3.32	−14	−4	70

activation patterns revealed no significant differences between frequencies.

The block-by-block analysis, performed to understand the pattern of deactivation for each stimulation time period over

the experimental run, revealed that the majority of the blocks for both 0.5 and 100 Hz demonstrated a reliable pattern of deactivation during “on” and relative activation during baseline (Fig. 3).

ROI analysis

We found no differences in mean thalamic activity when the device was “on” versus baseline for either the 0.5- or 100-Hz CES.

Current intensity regression

A voxel-wise analysis using current as a regressor revealed positive associations between current and activation for 100-Hz but not 0.5-Hz stimulation. Regions included right/left posterior cingulate cortex, left superior parietal lobule, left angular gyrus, left supramarginal gyrus, and left lateral occipital cortex (Table S2). There were no significant associations with brain deactivation in any region. This pattern for current intensity therefore differed from what was found in the “on” versus baseline analyses, suggesting that cortical deactivation may depend more on frequency than intensity of stimulation.

PPI analysis (Fig. 4 and Table 2)

For the DMN analysis, 100 Hz was associated with increased connectivity between the posterior cingulate cortex seed and the left planum temporale, bilateral postcentral gyrus, and

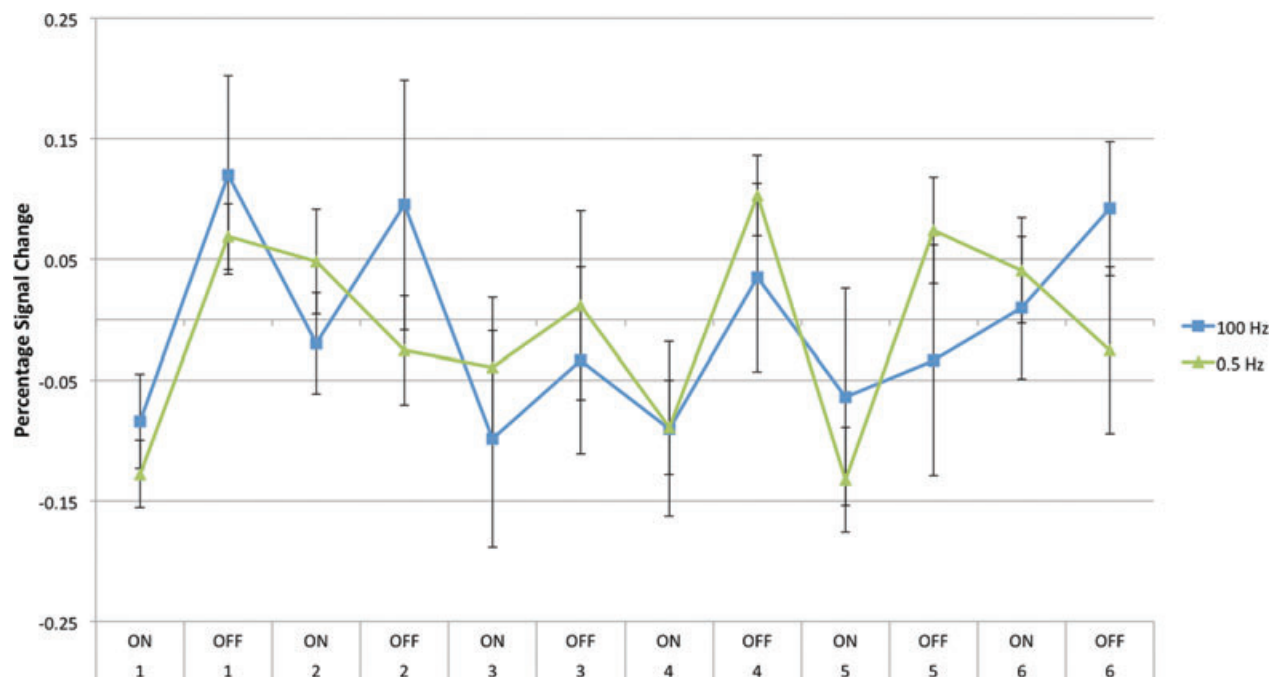


Figure 3. Time course of activation/deactivation block-by-block, averaged for regions for which there was overlap from all 11 participants' leave-one-subject-out group activation maps (see Fig. S1).

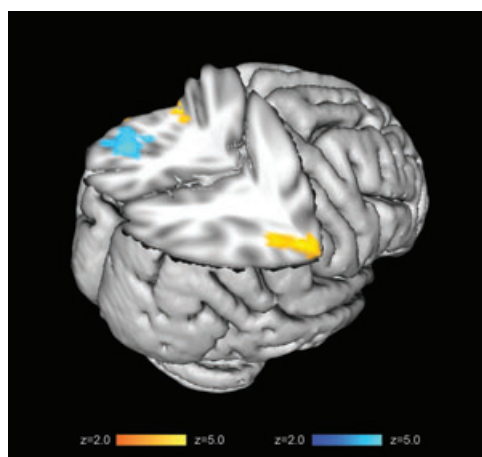


Figure 4. Regions of altered connectivity with the posterior cingulate seed within the default mode network associated with 100-Hz stimulation. Regions of increased connectivity are depicted in yellow–orange and decreased connectivity are depicted in blue–light blue.

Table 2. Regions of altered functional connectivity associated with CES stimulation at 100 Hz between the bilateral posterior cingulate gyrus (seed region) and other regions within the default mode network. Z scores and MNI coordinates for local maxima (x, y, z) are given.

Default mode network				
Region	Z score	x	y	z
Increased connectivity				
Left planum temporale	3.87	−52	−34	14
Right postcentral gyrus	3.56	66	−14	14
Left supramarginal gyrus, anterior	3.48	−68	−26	24
Left postcentral gyrus	3.4	−68	−22	24
Right supramarginal gyrus, anterior	2.89	58	−26	32
Decreased connectivity				
Left supramarginal gyrus, posterior	3.34	−42	−44	34
Left angular gyrus	3.18	−38	−58	40
Left lateral occipital cortex, superior	2.59	−48	−62	50

bilateral anterior supramarginal gyrus (Fig. 4 and Table 2). A total of 100 Hz was also associated with decreased connectivity between the posterior cingulate cortex seed and the left posterior supramarginal gyrus, the left angular gyrus, and the left superior lateral occipital cortex. A total of 0.5 Hz was not associated with any significant changes in connectivity. For the SMN, neither 100-Hz nor 0.5-Hz stimulation was associated with any significant changes in connectivity. For the FPN, there were no significant alterations of connectivity detected for either frequency.

Discussion

Results from this study suggest that 0.5- and 100-Hz CES causes cortical brain deactivation in midline prefrontal and

parietal regions. In addition, 100-Hz stimulation significantly altered connectivity within the DMN. CES thus appears to result in similar cortical deactivation patterns for 0.5- and 100-Hz, but is associated with stronger alterations in functional connectivity for 100-Hz stimulation. Moreover, cortical deactivation patterns differed from those associated with current intensity, suggesting that cortical deactivation may depend more on frequency than intensity of stimulation.

These results may help shed light on potential mechanisms of action of CES. Previously proposed mechanisms have included changes in brain oscillation patterns, neurotransmitter and endorphin release, interruption of ongoing cortical activity, or secondary effects from peripheral nerve stimulation (Zaghi et al. 2009). These proposed mechanisms may not be mutually exclusive. For example, the oscillating current from CES may reach the cortex where it may interrupt normal resting state cortical activity, resulting in deactivation. In doing so, CES may alter brain oscillation patterns. The observation of reduced BOLD signal associated with stimulation in the current study fits with previous EEG studies of CES that demonstrated downward shift in mean or median alpha frequency with stimulation (Itil et al. 1972; Schroeder and Barr 2001), as lower frequency brain activity has been found to be associated with lower BOLD signal in studies of simultaneous colocalized electrophysiological and fMRI recordings (Magri et al. in press) and in epilepsy (Archer et al. 2003). The different alterations in connectivity observed in this study with 100-Hz relative to 0.5-Hz stimulation could be related to the overlapping but somewhat differential effects of these frequencies on EEG patterns found in previous studies (Schroeder and Barr 2001). The observation that 100-Hz but not 0.5-Hz stimulation significantly affected connectivity in the DMN in this study may be related to previous observations that 100-Hz but not 0.5-Hz affects the beta band, which has been found to correlate strongly with activity in the DMN (Mantini et al. 2007; Laufs 2008).

In regards to how the current reaches the brain, because this study used earlobe electrodes, the alternating microcurrent may initially stimulate afferent branches of cranial nerves. Stimulation may initially occur at branches of the facial, glossopharyngeal, and/or the vagus nerves that originate near the electrode placement on the earlobe, then are carried to the brainstem, the thalamus, and finally the cortex.

Two different clinically effective frequencies (100 or 0.5 Hz) were associated with brain deactivation, but the amplitude of current was not. This provides additional mechanistic evidence that CES may exert its effects through interruption of normal cortical activity, possibly through the introduction of high- or low-frequency noise that interferes with certain brain oscillation patterns.

The results of this study may have several important clinical implications. Applying AC to the brain at different

frequencies may alter communication between nodes of the DMN. Studies in clinical populations, including anxiety disorders and depression, have found abnormalities in these intrinsic connectivity networks (for review see [Broyd *et al.* 2009]). One study found that anxiety disorder patients, when presented with threat-related words, demonstrated decreased activity in regions that overlap with the DMN including the posterior cingulate cortex (PCC) and inferior parietal lobule, as well as medial prefrontal cortex and thalamus (Zhao *et al.* 2007). Liao *et al.* (2010) found decreased functional connectivity in individuals with social anxiety disorder within the SMN and DMN (Liao *et al.* 2010). In addition, individuals with both acute (Mantini *et al.* 2009) and chronic pain (Baliki *et al.* 2008) have been shown to have abnormal functional connectivity in the DMN.

How the specific effects of CES on brain deactivation and on intrinsic connectivity networks translate to impacting clinical symptoms still remains to be investigated. In patients with anxiety and those with depression, one possibility is that alterations of the DMN may have a therapeutic effect of disengaging worry- or rumination-promoting internal dialogue (Hamilton *et al.* 2011) and/or promoting attention to external stimuli. One way this may occur is that increasing connectivity within the DMN between the PCC and supra-marginal gyrus and postcentral gyrus (as found in this study) may lead to increased integration of external sensory information (Bear 1983). With an improved understanding of these processes, it may be possible that CES parameters such as frequency could be tuned for individuals to therapeutically target different connections within abnormally functioning intrinsic connectivity networks.

This study has several limitations to consider. The small sample size may have resulted in insufficient power to detect smaller changes in resting brain activity. Another limitation is that we did not use a pure sham condition. Rather, we tested sensory thresholds prior to scanning to ensure that participants could not detect if the stimulation was on or off, effectively incorporating control blocks (used as “baseline”) within the experimental design, from which to compare to “on” stimulation blocks. Although we used these same individualized subsensory currents during the experiment, we did not have an accurate way of verifying if participants perceived the stimulation during the scan block by block, as this would have interrupted the “resting state” nature of the experiment. However, questioning participants after the scan revealed that only one participant reported feeling a constant (nonalternating) “sensation” on the left earlobe, which was inconsistent with the pattern of CES used in the experiment and instead likely due to the pressure of the headphone. Another limitation comes from the fact that the stimulation was brief and intermittent in this experiment, limiting the ability to extrapolate findings to changes over longer durations of treatment. In addition, since this was a nonclinical sam-

ple, anxiety levels were low before and after stimulation; this limits the ability to understand immediate effects, if any, on this symptom domain. Similar studies in clinical populations are needed to further elucidate how cortical deactivation and changes in intrinsic connectivity networks may translate to therapeutic mechanisms of action.

Conclusions

This study provides evidence that CES stimulation may result in cortical deactivation, as well as altering brain connectivity in the DMN. This suggests that relatively small perturbations in brain oscillation patterns may cause significant changes in brain activity and within intrinsic connectivity networks. Findings from this study provide evidence of the mechanism of action of CES and can serve as a guide for testing in treatment trials in clinical populations. Optimizing CES parameters for effective treatment can then be developed based on how specific brain systems and pathways may modulate clinical states such as anxiety, pain, or insomnia.

Acknowledgments

Funding provided by a grant from the Saban Family Foundation (Bystritsky). This work was also supported by a grant from the National Institute of Mental Health (5K23 MH079212—Feusner). The authors would like to thank M. Burock for his input on the study design, and E. Pierce, J. Alger, and J. Kaplan for their assistance with safety and artifact testing in the MR scanner.

Conflict of Interest

None of the authors have any conflicts of interest to report.

References

- Aguirre, G. K., E. Zarahn, and M. D’Esposito. 1998. The variability of human, BOLD hemodynamic responses. *Neuroimage* 8:360–369.
- Archer, J. S., D. F. Abbott, A. B. Waites, and G. D. Jackson. 2003. fMRI “deactivation” of the posterior cingulate during generalized spike and wave. *Neuroimage* 20:1915–1922.
- Baliki, M. N., P. Y. Geha, A. V. Apkarian, and D. R. Chialvo. 2008. Beyond feeling: chronic pain hurts the brain, disrupting the default-mode network dynamics. *J. Neurosci.* 28:1398–1403.
- Banquet, J. P. 1973. Spectral analysis of the EEG in meditation. *Electroencephalogr. Clin. Neurophysiol.* 35:143–151.
- Bear, D. M. 1983. Hemispheric-specialization and the neurology of emotion. *Arch Neurol.* [Review] 40:195–202.
- Beckmann, C. F., M. Jenkinson, and S. M. Smith. 2003. General multilevel linear modeling for group analysis in FMRI. *Neuroimage* [Article] 20:1052–1063.

- Bianco, F. 1994. The efficacy of cranial electrotherapy stimulation (CES) for the relief of anxiety and depression among polysubstance abusers in chemical dependency treatment. University of Tulsa, Tulsa, OK.
- Broyd, S. J., C. Demanuele, S. Debener, S. K. Helps, C. J. James, and E. J. Sonuga-Barke. 2009. Default-mode brain dysfunction in mental disorders: a systematic review. *Neurosci. Biobehav. Rev.* 33:279–296.
- Buckner, R. L., J. R. Andrews-Hanna, and D. L. Schacter. 2008. The Brain's default network: anatomy, function, and relevance to disease. *Ann. NY Acad. Sci.* 1124:1–38.
- Bystritsky, A., L. Kerwin, and J. Feusner. 2008. A pilot study of cranial electrotherapy stimulation for generalized anxiety disorder. *J. Clin. Psychiat.* 69:412–417.
- Corbetta, M., and G. L. Shulman. 2002. Control of goal-directed and stimulus-driven attention in the brain. *Nat. Rev. Neurosci.* 3:201–215.
- De Luca, M., C. F. Beckmann, N. De Stefano, P. M. Matthews, and S. M. Smith. 2006. fMRI resting state networks define distinct modes of long-distance interactions in the human brain. *Neuroimage* 29:1359–1367.
- DeFelice, E. A. 1997. Cranial electrotherapy stimulation (CES) in the treatment of anxiety and other stress-related disorders: a review of controlled clinical trials. *Stress Med.* 13:31–42.
- Esterman, M., B. J. Tamber-Rosenau, Y.-C. Chiu, and S. Yantis. 2010. Avoiding non-independence in fMRI data analysis: leave one subject out. *Neuroimage* 50:572–576.
- Friston, K. J., C. Buechel, G. R. Fink, J. Morris, E. Rolls, and R. J. Dolan. 1997. Psychophysiological and modulatory interactions in neuroimaging. *Neuroimage* 6:218–229.
- George, M. S., Z. Nahas, J. J. Borckardt, B. Anderson, M. J. Foust, C. Burns, S. Kose, E. B. Short. 2007. Brain stimulation for the treatment of psychiatric disorders. *Curr. Opin. Psychiat.* 20:250–254; discussion 47–49.
- Gilula, M. F. 2007. Cranial electrotherapy stimulation and fibromyalgia. *Expert Rev. Med. Dev.* 4:489–495.
- Hamilton, J. P., D. J. Furman, C. Chang, M. E. Thomason, E. Dennis, and I. H. Gotlib. 2011. Default-mode and task-positive network activity in major depressive disorder: implications for adaptive and maladaptive rumination. *Biol. Psychiat.* 70:327–333.
- Itil, T., P. Gannon, S. Akpinar, and W. Hsu. 1972. Quantitative EEG analysis of electrosleep using analog frequency analyzer and digital computer methods. *Dis. Nerv. Syst.* 33:376–381.
- Jarzembski, W., and A. J. Sances. 1970. Evaluation of specific cerebral impedance and cerebral current density. *Ann. NY Acad. Sci.* 170:476–490.
- Jarzembski, W. B. 1985. Electrical stimulation and substance abuse treatment. *Neurobehav. Toxicol. Teratol.* 7:119–123.
- Jenkinson, M., and S. Smith. 2001. A global optimisation method for robust affine registration of brain images. *Med. Image Anal.* 5:143–156.
- Jenkinson, M., P. Bannister, M. Brady, and S. Smith. 2002. Improved optimization for the robust and accurate linear registration and motion correction of brain images. *Neuroimage* 17:825–841.
- Jensen, A. L., and D. M. Durand. 2007. Suppression of axonal conduction by sinusoidal stimulation in rat hippocampus in vitro. *J. Neural Eng.* 4:1–16.
- Kirsch, D. L. 1996. Cranial electrotherapy stimulation: a safe and effective treatment for anxiety. *Med. Scope Mon. (Alberta)* 3:1–26.
- Klawansky, S., A. Yeung, C. Berkey, N. Shah, H. Phan, and T. C. Chalmers. 1995. Meta-analysis of randomized controlled trials of cranial electrostimulation. Efficacy in treating selected psychological and physiological conditions. *J. Nerv. Ment. Dis.* 183:478–484.
- Laufs, H. 2008. Endogenous brain oscillations and related networks detected by surface EEG-combined fMRI. *Hum. Brain Mapp.* 29:762–769.
- Liao, W., H. F. Chen, Y. A. Feng, D. Mantini, C. Gentili, Z. Y. Pan, *et al.* 2010. Selective aberrant functional connectivity of resting state networks in social anxiety disorder. *Neuroimage [Article]* 52:1549–1558.
- Magri, C., U. Schridde, Y. Murayama, S. Panzeri, and N. Logothetis. 2012. The amplitude and timing of the BOLD signal reflects the relationship between LFP power at different frequencies. *J. Neurosci.* 32:1395–1407.
- Mantini, D., M. G. Perrucci, C. Del Gratta, G. L. Romani, and M. Corbetta. 2007. Electrophysiological signatures of resting state networks in the human brain. *Proc. Natl. Acad. Sci. USA* 104:13170–13175.
- Mantini, D., M. Caulo, A. Ferretti, G. L. Romani, and A. Tartaro. 2009. Noxious somatosensory stimulation affects the default mode of brain function: evidence from functional MR imaging. *Radiology [Article; Proceedings Paper]* 253:797–804.
- O'Connell NE, B. M. Wand, L. Marston, S. Spencer, and L. H. DeSouza. 2010. Non-invasive brain stimulation techniques for chronic pain. *Cochrane Database Syst. Rev. [Review]* 9:1–82.
- Rush, S., and D. A. Driscoll. 1968. Current distribution in the brain from surface electrodes. *Anesth. Analg. Curr. Res.* 47:717–723.
- Schopf, V., C. H. Kasess, R. Lanzenberger, F. Fischmeister, C. Windischberger, and E. Moser. 2010. Fully exploratory network ICA (FENICA) on resting-state fMRI data. *J. Neurosci. Meth.* 192:207–213.
- Schroeder, M. J., and R. E. Barr. 2001. Quantitative analysis of the electroencephalogram during cranial electrotherapy stimulation. *Clin. Neurophysiol.* 112:2075–2083.
- Sheehan, D. V., Y. Lecrubier, K. H. Sheehan, P. Amorim, J. Janavs, E. Weiller, *et al.* 1998. The Mini-International Neuropsychiatric Interview (M.I.N.I.): the development and validation of a structured diagnostic psychiatric interview for DSM-IV and ICD-10. *J. Clin. Psychiat.* 59:22–33.
- Shulman, G. L., J. A. Fiez, M. Corbetta, R. L. Buckner, F. M. Miezin, M. E. Raichle, *et al.* 1997. Common blood flow

- changes across visual tasks. 2. Decreases in cerebral cortex. *J. Cogn. Neurosci.* 9:648–663.
- Southworth, S. 1999. A study of the effects of cranial electrical stimulation on attention and concentration. *Integr. Physiol. Behav. Sci.* 34:43–53.
- Spielberger, C., R. Gorsuch, P. Lushene, and P. Vagg. 1983. *AG J. Manual for the State-Trait Anxiety Inventory (Form Y)*. Consulting Psychologists Press, Inc., Palo Alto, CA.
- Spreng, R. N., W. D. Stevens, J. P. Chamberlain, A. W. Gilmore, and D. L. Schacter. 2010. Default network activity, coupled with the frontoparietal control network, supports goal-directed cognition. *Neuroimage* 53:303–317.
- Sridharan, D., D. J. Levitin, and V. Menon. 2008. A critical role for the right fronto-insular cortex in switching between central-executive and default-mode networks. *Proc. Natl. Acad. Sci. USA* 105:12569–12574.
- Tan, G., D. H. Rintala, M. P. Jensen, J. S. Richards, S. A. Holmes, R. Parachuri, *et al.* 2011. Efficacy of cranial electrotherapy stimulation for neuropathic pain following spinal cord injury: a multi-site randomized controlled trial with a secondary 6-month open-label phase. *J. Spinal Cord Med.* 34:285–296.
- Uddin, L. Q., A. M. Kelly, B. B. Biswal, F. Xavier Castellanos, and M. P. Milham. 2009. Functional connectivity of default mode network components: correlation, anticorrelation, and causality. *Hum. Brain Mapp.* 30:625–637.
- Woolrich, M., M. Brady, and S. Smith. 2001. Hierarchical fully Bayesian spatio-temporal analysis of fMRI data. Seventh International Conference on Functional Mapping of the Human Brain, Brighton, U.K.
- Worsley, K. J. 2001. Statistical analysis of activation images. Pp. 251–270 *in* P. Jefferard, P. M. Matthews, and S. M. Smith, eds. *Functional MRI: an introduction to methods*. Oxford, OUP.
- Zaghi, S., M. Acar, B. Hultgren, P. S. Boggio, and F. Fregni. 2009. Noninvasive brain stimulation with low-intensity electrical currents: putative mechanisms of action for direct and alternating current stimulation. *Neuroscientist* 16:285–307.
- Zhao, X. H., P. J. Wang, C. B. Li, Z. H. Hu, Q. Xi, W. Y. Wu, *et al.* 2007. Altered default mode network activity in patient with anxiety disorders: an fMRI study. *Eur. J. Radiol.* 63:373–378.

Supporting Information

Additional Supporting Information may be found in the online version of this article:

Figure S1. Group results from the leave-one-subject-out analyses.

Table S1. Demographic data, sensory threshold testing results, and current intensities.

Table S2. Local maxima for regions positively associated with current intensity for 100-Hz CES stimulation.

Please note: Wiley-Blackwell is not responsible for the content or functionality of any supporting materials supplied by the authors. Any queries (other than missing material) should be directed to the corresponding author for the article.